

Development of a high resolution topography and color scanner to capture crack patterns of paintings

M.J.W. van Hengstum¹, T.T.W. Essers², W.S. Elkhuizen², D. Dodou¹, Y. Song², J.M.P. Geraedts², and J. Dik³

¹TU Delft, Biomechanical Engineering, The Netherlands, ²TU Delft, Design Engineering, The Netherlands
³TU Delft, Materials Science and Engineering, The Netherlands

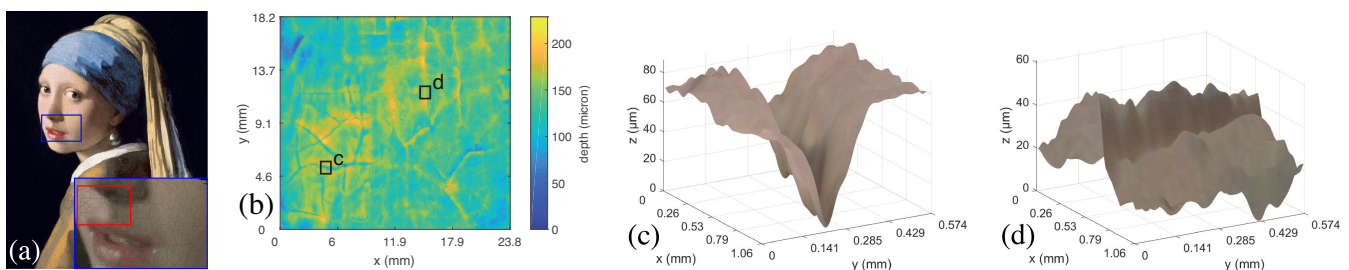


Figure 1: The crack pattern of the painting *Girl with a Pearl Earring* by Johannes Vermeer was captured. The red square in (a) highlights the sampled scan region, of which the height map is depicted in (b). Image (b) also marks the regions which are rendered in (c) and (d).

Abstract

The aging of paintings is inevitable and over the years degradation occurs due to exposure to a variety of environmental influences. One of these degradations is craquelure, fracture patterns in the paint. 3D imaging techniques offer opportunities to capture the surface of a painting and these patterns at high resolution. In this paper we present a 3D scanner that is able to capture surface topography and color of oil paintings at high resolution utilizing fringe-encoded stereo imaging scanning system. The scanner is capable of automated capture of an area of 1x1m², capturing a painting at a spatial resolution of 7 micron and a depth accuracy of 34 microns. Scanning at this resolution creates potential research opportunities for documentation and monitoring oil paintings under its environmental influences. A scan was made of 'Girl with a Pearl Earring' (c.1665), painted by Johannes Vermeer, which exhibits fine craquelure patterns. The scanner is able to capture the painting of 39x44.5 cm within 2 hours with a tile overlap of 25%. The results showed that the craquelure has more often a ridge-shaped profile instead of the expected inward valleys. The documentation of these variations in crack profiles create interesting paths for future research.

CCS Concepts

•Computing methodologies → Point-based models; •Applied computing → Fine arts;

1. Introduction

Although museums and conservators go to great lengths to conserve treasured heritage, gradual aging of artifacts is unfortunately inevitable. In paintings, degradation can lead to, for instance, discolorations, migration of materials to the surface, crack formation, and even paint delamination. Many of these effects affect the three-dimensional shape of the surface. To support conservation efforts, it would be very useful to be able to document, monitor, and analyze the three-dimensional shape of the surface.

Stereo-microscopy allows conservators to examine the surface of a painting. Small fragments of paint can also be examined under a stereo microscope at different wavelengths; for instance, UV fluorescence can be used to distinguish the boundaries between varnish and paint [JBC96]. However, these individual samples do not provide conservators with a three-dimensional image of the complete painting. Digital 3D confocal microscopy has been applied to scan small areas of paintings at high magnification; unfortunately, it can take multiple days to scan even a small painting [Van18b].

3D scanning technologies complement ultra-high resolution 3D microscopy, in that they make it possible to scan the three dimensional surface of a complete painting within a realistic timeframe. For instance, Blais et al. developed a RGB-laser based system with a spatial resolution of 60 μm and depth uncertainty of 10 μm , used to scan the complete surface of the painting *Mona Lisa* by Leonardo da Vinci [BTC*]. 3D scanning and printing techniques based on fringe encoded stereo vision, have since then enabled museums to document the 3D shape of the painting, and create 3D printed reproductions of famous oil paintings [ZJLD14, EZV*14].

These topography and color imaging systems are capable of capturing the global 3D shape of a painting's surface as well as the fine brush strokes, which can support the description and documentation of the color usage, style and work flow of the painter [SSD08]. An even higher resolution scanner would potentially enable the documentation of even smaller details, like the craquelure pattern of oil paintings. Current state-of-the-art devices either lack the scanning planar range or the resolution to capture fine details like the craquelure pattern of the entire painting.

In this paper, a novel high-resolution topography and color scanner is introduced, based on fringe aided stereo imaging, capable of capturing the craquelure pattern of an entire painting. The paper describes the design requirements for a high-resolution topography and color scanner, and validates the resolution and accuracy of the system in terms of topography and color. A case study was conducted to test the capabilities of capturing fine surface details, scanning *Girl with a Pearl Earring* (c.1665) by Johannes Vermeer, in the collection of the Mauritshuis in the Hague, The Netherlands. Additionally another painting was used to determine the depth accuracy, by comparing the depth measurements of the scanner to 3D microscopy measurements. This paper is structured as follows: the remainder of section 1 describes what is known about craquelure patterns of paintings, which is followed by the design requirements for the scanning system. Section 2 describes relevant 3D scanning technologies which have been applied to capture the three dimensional shape of a painting's surface. In section 3 the scanner hardware is described. An overview of the calibration and capturing workflow is given in section 4, as well as the methods used to determine the spatial resolution, depth accuracy, color accuracy, and speed of the system. Section 5 describes the obtained results, and section 6 and 7 provide the discussion and conclusion, respectively.

1.1. Case Study

In 2018, the research project *The Girl in the Spotlight* focused on the materials and techniques used to paint the world famous painting *Girl with a Pearl Earring*. This research was for the most part non-invasive, whereby multiple imaging technologies were deployed to capture information about the surface and underlying layers of the painting [Van18a, BBC18]. The scanning system described in this paper was also used to visualize the surface. The characteristics of this painting and case study served as input for the design requirements of the scanner, although we envision more applications of the system in the future as it is suitable for capturing oil paintings with a maximum dimension of 1x1m.

Girl with a Pearl Earring was painted by Johannes Vermeer and

is dated around 1665. The size of the painted surface is 39x44.5 cm, and the craquelure is very fine and primarily rectangular shaped as a result of aging [Buc97a]. The fine cracks make the painting a suitable subject to test the capability to capture craquelure for the entire painting.

1.2. Craquelure Patterns in Paintings

Many paintings suffer from fractures in the paint and varnish layers. These fracture patterns - called cracks, crackle, or craquelure - can be caused by aging, drying, and mechanical factors. The crack pattern is one of the main factors in determining the quality of a painting and is a broad indicator of authorship [Buc97b, Lei96]. Moreover, delamination of the paint from the canvas often takes place at the edge of craquelure [OBSG10]. Therefore, being able to monitor the craquelure in the entire painting is a valuable tool for conservators and restorers to determine the quality of the painting and possible preserving procedures [SR13, Lau05].

The condition of a painting is also related to its response to environmental influences, like the humidity, light and temperature [Roc05, SJ13]. An accurate estimation of the craquelure would aid to objectively investigate these environmental influences on the degradation of a painting. Moreover, the finer craquelure is of great interest with respect to the detection of transportation damages [BCD*92]. For example, a proprietor of a painting could register the craquelure of the painting before and after transportation, to evaluate its effects. Even though craquelure is a prominent feature of the painting, there is little research on the exact dimensions of the cracks. Literature on craquelure in paintings, is primarily about the classification on the type of craquelure and the type of (2D) patterns they create [Buc00].

In the study of craquelure, combining color with topography information will provide a more complete understanding of the different features in the painting [ASC*13]. For example, this method, combined with color information can be used to differentiate between a sudden increase of paint height related to a crack, a thick blob of paint or excess dirt. The relation between topography and color helps restorers and conservators to monitor, visualize, and understand features in the painting [MP04].

1.3. Design Requirements for a High Resolution 3D Scanner

There are few general references on the exact dimension of the craquelure of *Girl with a Pearl Earring*. The initial estimation is based on the research data from the examination of the painting in 1994 [Mau94]. Through examination of existing high-resolution images of the painting and cross-sections of paint samples, it is estimated that the width of a craquelure varies between 50 to 100 μm , and the paint layer thickness between 25 to 300 μm . The profile of aging cracks, observed from an intersection of the paint layer, was described to approximate a rectangular shape [Buc97a].

To determine the spatial resolution and depth precision required to register the finest craquelure, sampling theorem was applied. To approximate a rectangular shape in signal analysis, the sampling frequency has to be minimally 5 times higher than the signal frequency [Bra86]. Since the width or wavelength of the signal is the

Table 1: Design requirements for high resolution topography and color scanner

Spatial Resolution (XY)	<10 μm
Depth Resolution (Z)	<5 μm
Acquisition Time (0.5m ²)	<8 hours
Color Accuracy	avr. <3 ΔE -2000 max. <6 ΔE -2000

inverse of the frequency, the width of the sampling signal has to be 5 times smaller than the width of the craquelure to register the shape. Applying this to describing the finest craquelure of 50 μm wide would require a spatial resolution of 10 μm (XY). Similarly, a depth precision of 5 μm is required to describe the depth of the shallowest crack. These requirements are easily met with the capabilities of 3D microscopes [FKK*07] and just beyond the capabilities of most full painting scanners based on digital photography, which can achieve a spatial resolution of approximately 25 μm [EEL*17].

The range of the XY-stage should enable the scanner to capture the surface of most paintings, where we estimate 90% of paintings is smaller than 60-by-80 cm, giving an area of roughly 0.5 m² [SSdD*09].

The time available at museums is often the limiting factor in scanning entire paintings. In ideal cases a working day or night of 8 hours is allocated to scan the artwork. However, the acquisition time is difficult to determine since it varies with the painting size, the type of device, the resolution and device settings. In general, the high resolution scanners, like 3D microscopes, require multiple days to scan an entire painting. High resolution scanning is generally accompanied with long acquisition time since more information has to be captured for the same area. Therefore, the acquisition time should be reduced, while preserving high resolution. The design requirements of the high resolution scanner are set to scan the painting within 8 hours. Up to recently techniques based on digital photography have a lower resolution and are capable of scanning a painting within 8 hours [EEL*17]. However also this can greatly vary with the implementation, influenced by many factors, e.g. the chosen illumination and camera settings.

As we aim to develop a painting documentation tool, it is desirable to comply to archiving guidelines for color imaging. Guidelines set by the Federal Agencies Digital Guidelines Initiative (FADGI) state that for the highest performance level, an accurate color reproduction is achieved when the average color error is lower than 3 ΔE -2000, with the maximum error below 6 ΔE -2000 [Fed10], which we therefore adopt as a design requirement.

The design requirements for a scanner capable of capturing the craquelure pattern of *Girl with a Pearl Earring* are summarized in table 1.

2. Scanning Technologies for Capturing Painting Surfaces

Various technologies have been implemented for capturing the topography and color of paintings. The potential of techniques capable of capturing craquelure patterns of a painting's surface are discussed below.

Digital 3D confocal microscopy can achieve a sub-micron resolution, but it requires the depth of field to be as small as possible to determine the depth accurately [FKK*07]. The depth of field is the area parallel to the capturing device that is in focus. A small depth of field is achieved by increasing the magnification, which in turn increases the acquisition time, as each tile only captures a very small area of the painting [Tow94]. At a magnification of 140x, which is needed to construct a 3D image, a large stack of images is needed per tile where the tile size is only about 5mm². The tiles then have to be stitched together to construct an image of the entire painting.

However, literature study indicates that there is limited research about using confocal microscope to capture an entire painting at a size comparable to our case study painting [Van18b]. Apart from a long acquisition time and limited range, a confocal microscopy is an expensive device.

Photogrammetry is widely used to determine the dimensions of 3D objects due to its user-friendliness [BFM*13]. The limitation is the dependence on having to match areas to determine the camera position and orientation relative to the previous location and then also reconstruct the 3D image on these matched areas. Areas that do not have sufficient features to match, like the background in a painting, can not be reconstructed [LRKH06]. The technique is economical since it only requires one camera, but the depth precision is limited to 50 μm with the current technology [Pho17].

Photometric stereo imaging estimates the depth from the shadows and highlights created by varying the direction of the incident lights [OS17]. An algorithm extracts the shade and highlights from the multiple images and estimates the depth from the shape. The angle of the incident light influences the trade-off between the depth precision and the depth estimation of craquelure, since larger shadows increase the depth precision, but decrease the ability to register cracks [Woo80]. The primary issue of using photometric stereo imaging is the depth precision, since the shadow and highlights are difficult to extract and do not always describe the topography of the painting accurately [BP03]. Photometric stereo imaging needs a camera and several light sources, making it an economical technique.

Fringe-encoded stereo imaging determines the depth by using triangulation with two cameras. Fringe projection uniquely labels each position on the painting to aid the triangulation and solve the correspondence problem in photogrammetry. In contrast to confocal microscopy, this technique requires a large depth of field - meaning that everything within one tile should be in focus - to determine depth, reducing the required spatial resolution and thus the acquisition time. Fringe-encoded stereo imaging uses two cameras and is therefore more expensive than other single camera techniques.

Scanners based on this technology have been used to produce a 3D printed reproduction of a painting. Reproducing a painting, perceptually equal for humans to the real painting, requires a spatial resolution of approximately 50 μm [CSKH90] (600 dpi means pixel width is about 42.33 μm). Current scanners therefore have specifications of a spatial resolution of 25 μm , a depth precision of 10 μm and acquisition time of 4 minute per tile [ZJLD14], which do not

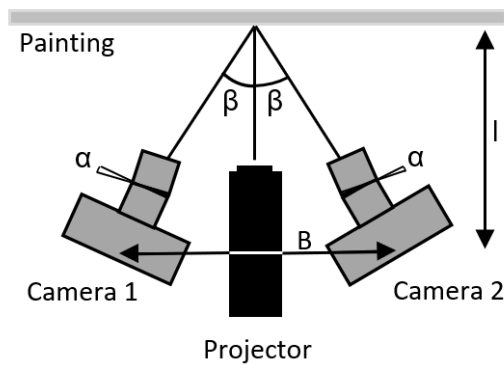


Figure 2: The setup of fringe encoded stereo imaging as seen from a top view. The cameras are placed 200 mm (l) from the painting with 140 mm (B) spacing between the cameras. The optical axis of the cameras relative to the painting's normal vector is 21.5° (β). The tilt-shift lenses are tilted by 8° (α) to align the focal plane with the painting's surface.

meet the requirements to scan the craquelure. However, the technique can potentially reach a higher resolution and be more accurate when adapting the hardware and software.

3. Materials

Existing scanning devices (e.g. [EEL*17]) based on fringe encoded stereo imaging devices currently lack the resolution required to capture the fine craquelure patterns. To meet the requirements, changes were made at both the hardware and the software. The changes in the hardware were focused at increasing the spatial resolution. The depth accuracy changes proportionally with the spatial resolution when the camera angles relative to the painting's normal vector remain equal, based on the geometry in stereo imaging. The existing software was adjusted to reduce the acquisition time, keeping in mind that the acquisition time scales two-dimensionally with a change in resolution.

The hardware consists of two cameras, a projector and a linear XY-stage, which translates the device parallel to the painting (see figure 3). All components are adapted (with regards to the Elkhuisen et al. [EEL*17] implementation) to enhance the spatial resolution, but also lower the acquisition time. A schematic overview of the hardware is shown in Figure 2 and the hardware changes are summarized in Table 2.

3.1. Cameras and tilt-shift lenses

The key specifications of the camera and lens are: the amount of pixels of the camera sensor, the pixel pitch, and the magnification of the lens. An increase in amount of pixels increases the tile size, which determines the number of tiles required to scan the painting and thus the acquisition time. The pixel pitch is the distance from pixel center to its neighbour's center and thus directly affect the spatial resolution. The magnification of the image is primarily determined by the camera lens. Moreover, the camera angle relative to the painting's normal vector (β in Figure 2) and the spatial

resolution determine the theoretical depth precision. Increasing the camera angle enhances the depth precision, but it makes the scanner more susceptible to occlusions.

Two Canon EOS 5Ds cameras, both able to capture images at the resolution of 50.6 mega pixels, were used with 90mm TS-E f/2.8 tilt-shift lenses (tilt angle α in Figure 2). Given the distance between the camera and the painting (200 mm), and a pitch of $4.1 \mu\text{m}$ a spatial resolution of $15.4 \mu\text{m}$ can be achieved. In addition, a 25 mm extension tube is placed between the camera and the lens to theoretically achieve a spatial resolution of $7 \mu\text{m}$. An extension tube magnifies the image by elongating the divergence of the light without compromising on the quality. However, the longer divergence results in less light striking the sensor, thereby requiring a longer exposure time to compensate the loss of light and thus increases the acquisition time (+20%). Moreover, the increased spatial resolution reduces the tile size to $60 \times 40 \text{ mm}$, as well as reducing the depth of field of the cameras. A smaller depth of field increases the difficulty to get the entire surface of the painting in focus for the cameras. The magnification also results in a smaller camera working distance (l in Figure 2), which means that the cameras have to be placed closer to each other. A consequence of this is that the space between the cameras (B in Figure 2), where the projector should be positioned, also becomes smaller.

To reduce the amount of potential occlusions, and to be able to align the depth of field with the painting plane, the camera angle (β in Figure 2) was decreased from 40° (in the design of [Zam13]) to 21.5° in the new system.

3.2. Projector

The important specifications of a projector are: the dimensions, intensity, and throw distance. The projector should fit between the cameras in order to perpendicularly project the fringe pattern and to limit the shape distortions from the projector lens and also reduce the shading on the painting's surface. A high intensity projector reduces the influence of the environmental lighting and more importantly reduces the required exposure time and thus the acquisition time. The working distance depicts the required throw distance of the projector, which is about 200 mm for the selected hardware.

The Acer X113H (2800 Lumens) projector, with a high pressure mercury lamp as illuminant, was replaced with the AXAA M6 (1200 Lumens) LED pico-projector, to meet the short throw distance and the dimensional requirements. The pico-projector is smaller, but it still has to be rotated 90° to fit between the cameras. The pico-projector with the highest available intensity was selected. This means that projection intensity was sacrificed to be able to fit the projector between the cameras and be able to focus at the working distance. This increased the exposure time from 0.5s to 0.6s and thus the minimal acquisition time (+20%). Moreover, polarization filters are applied to the cameras and projector, to achieve cross polarization in order to remove any specularities introduced by the projector or the surface of the painting.

3.3. XY-stage

The important parameters of a XY-stage are: its positioning precision, range, rigidity, and portability. The XY-stage needs to pre-

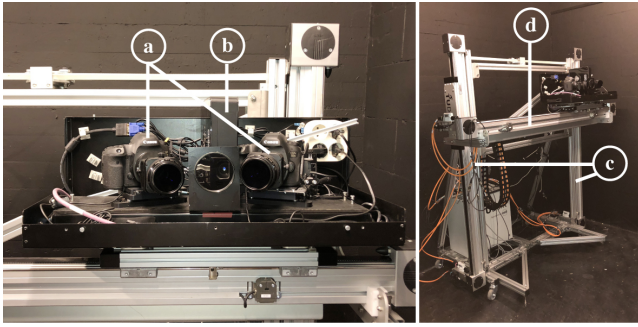


Figure 3: The XY-stage translates (a) the two cameras and (b) projector parallel to the painting, (c) two vertical linear drivers and (d) a horizontal linear driver provide the precise, automated movement, while minimizing the vibrations with a rigid structure.

cisely translate the scanner parallel to the surface of the painting, to ensure the overlap is consistent. The required precision depends on the tile size and the minimal overlap. The selected hardware results in a tile size of 60x40 mm and a minimal overlap of 25% (10mm) to be able to stitch the images together. This results in a minimal precision of 1.0 mm to position the scanner with sufficient certainty. The stage also has to be rigid enough to minimize vibrations, while being portable to transport to any museum. The vibrations influence the quality and the consistency of the image, leading to, for instance, motion blurring, resulting in a lower effective resolution. A rigid XY-stage is therefore essential for accurate topography and color reproduction. The high precision and rigid XY-stage is depicted in Figure 3, which can be fully disassembled for transportation. Two linear drivers move the device vertically and one linear driver horizontally for a range of 1 by 1 meter with an effective precision of 0.01 mm. Moreover, the XY-stage is designed with a wide base to enhance the stability to minimize vibrations.

3.4. Hardware specification summary

The specifications of the fine art scanner by Elkhuizen et al. [EEL*17] and the new hardware are summarized in Table 2. The new hardware result in an estimated spatial resolution of 7 μm and depth accuracy of 5 μm , which is an increase of a factor 3.5 compared to the spatial resolution of the previous implementation. As mentioned, the acquisition time scales two-dimensionally with the resolution. Therefore, the acquisition time increases with a factor 12 (3.5^2). When taking the extension tube, pico-projector, and camera sensor into account the acquisition time is increased with a total factor of around 13. The validation method and results of these estimates can be found in Section 4 and Section 5, respectively.

4. Method

4.1. Calibration and scanning workflow

Figure 4 gives an overview of the workflow of the calibration and scanning procedure for capturing a painting, after the device is fully assembled.

The work flow starts with the camera settings, which determine

Table 2: Summary of specifications of the fine art scanner of Elkhuizen et al. [EEL*17] and our new scanner.

	Elkhuizen et al.	Our hardware
Camera model	Nikon D800E	Canon EOS 5Ds
Cam Resolution	36.3 MPixels	50.3 MPixels
Pixel pitch	4.87 μm	4.14 μm
Cam. Angle (β)	40 $^\circ$	21.5 $^\circ$
Camera Lens	Nikkor PC-E 85 mm	Canon TS-E 90 mm
Spatial Resolution	25 μm	7 μm
Depth Precision	10 μm	5 μm
Tile size	170x100 mm	60x40 mm
Projector model	Acer X113H	AXAA M6
Intensity	2800 Lumens	1200 Lumens
Resolution	800x600 px	1920x1080 px
XY-stage precision	± 1 mm	0.01 mm
Automated Range	1.3x1.3 m	1x1 m

the quality and salience of the image. The aperture is set to $f/16$, which is a trade-off between the depth of field and the exposure time and thereby total acquisition time, while at the same time keeping diffraction to a minimum. Higher ISO often introduces more noise. The ISO is therefore kept at the lowest possible setting (100) to minimize sensor noise, which is at the cost of longer exposure time. The exposure time is chosen based in the color calibration target, avoiding as much as possible under or over exposure of the target color patches. The XY-stage is positioned as parallel as possible to the painting at the working distance of 200mm for the cameras. The next step of the workflow is the calibration of the system, the cameras are calibrated using the camera calibration toolbox of Zhang et al. [Zha00] in a 2017a Matlab[®] implementation. Usually, the projector's position and orientation are calibrated for fringe projection, however fringe encoded stereo imaging bases its depth estimation on stereo imaging, eliminating the need for projector calibration. The last step before the scan is to set a custom white balance and to calibrate the color. An image of a grey chart is captured to set a custom white balance using the built-in software of the cameras. The color is calibrated with a micro color reference chart, to create a custom ICC-profile for the cameras, with the projector as the illuminant.

The capturing sequence, consists of capturing projected fringe patterns and moving to the next tile. The fringe projection is projected horizontally and vertically to acquire 3D information of the projected area. The projected fringe pattern is a sinusoidal pattern in greyscale that shifts with an off-set related to the amount of phases. A fringe pattern with a wavelength of 12 pixels and 6 phases obtained a more consistent result compared to the original 3 phases [Zam13], but also doubles the total images and the total acquisition time. One additional image is captured with a uniform illumination which is used for the color image data.

After the fringes have been captured, they are wrapped into a wrapped phase map. The phase map is unwrapped to generate the continuous phase map, uniquely labeling each position on the image. To correlate the cameras, about 1500 (the set threshold) features from both unwrapped maps are matched with the sparse

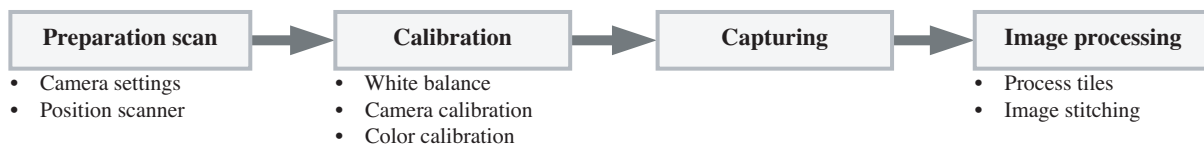


Figure 4: When the scanner is installed, all devices are set to the appropriate setting and calibrated. The white balance of the cameras are set, a color calibration is made as well as a geometric calibration. The painting is captured with 13 images per tile. After scanning the images are processed offline for each tile and finally stitched together to form an image of the total painting, also offline.

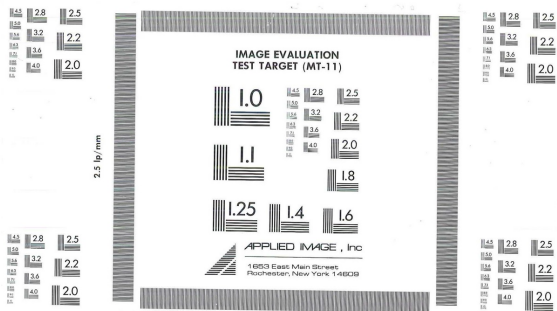


Figure 5: The Applied Image Inc. MT-11 MTF chart contains several arrays and small patches of fine lines with varying line densities. The long 2.5 line/mm MTF bars positioned as a larger square, are used to determine the spatial resolution of the scanner for different parts of the processed image.

matching algorithm SIFT [Low04]. The correlated phase maps match each unique value of both cameras, enabling the computation of the 3D position of each point. This position can be computed through ray tracing by taking into account the information from our camera calibration. The construction of this 3D point cloud takes about 15-30 minutes per tile in our MATLAB implementation, based on the implementation of Zaman et al. [ZJLD14].

4.2. Spatial Resolution

The spatial resolution of any imaging system is defined as its ability to distinguish two points as separate in space. In fringe encoded stereo imaging, the spatial resolution is the distance that neighbouring pixels capture of the real world object. Commonly, to determine this real world distance, an object with known spacing is captured and processed, for instance a ruler. In this study a MTF chart was used to determine the spatial resolution, which is a commonly used tool in (2D) digital photography. Figure 5 shows the Applied Image Inc. MT-11 MTF chart used to determine the spatial resolution. The MTF chart contains several arrays of fine bars, which are typically used to determine the quality of the camera lens. This chart is an effective method to determine the spatial resolution, since the number of pixels describing the known amount of bars per millimeter determines the spatial resolution [Oka97].

To determine the spatial resolution in horizontal (X) and vertical (Y) direction of the entire processed image, three horizontal and three vertical MTF bars with 2.5 lines per millimeter equally spaced

over the tile were captured. The amount of pixels of the processed image describing the distance between the lines is used to define the spatial resolution of the scanner.

4.3. Depth Accuracy

The depth accuracy is the ability to faithfully recreate the three-dimensional shape of the surface. In stereo imaging, the depth accuracy is largely determined by the spatial resolution and the camera angle (β in Figure 2). As the estimated depth resolution is expected to be around 18 μm , existing calibration plates cannot be easily made, with sufficient level of detail to determine the depth accuracy. Additionally, in order to calculate the topography the algorithm depends a certain level of salient features, and continuity of the surface. Existing calibration plates do not meet these constraints. The measured depth of the painting is therefore compared to a ground truth measurement.

The depth accuracy of the presented scanner is determined by comparing the depth measurements of our scanner to the more precise Bruker ContourGT-K Scanner, which has a depth precision (RMS repeat measurement) of 1 nm [Bru18], for the used sampling resolution. Both scanners capture the same three areas of a specially created section of a painting, shown in Figure 6. This section was cut from an old painting with fine craquelure and stuck to a wooden panel to eliminate deformations of the canvas when switching between devices. Three sections of 6.5x4.8 mm are imaged with the Bruker microscope, which are a composite of 3 by 3 individual measurements. The same regions are cropped from the scanner data, to match the area of the microscope images. The pixels which do not contain data (in both scanners) are excluded from the depth comparison. The depth maps of these three areas are digitally translated and rotated in the optimal orientation to compute the difference in depth between the two depth maps. For each of the three areas the depth difference is calculated and the standard deviation represents half of the depth accuracy.

4.4. Color Accuracy

The measurement of the colors is influenced by multiple factors, such as the illuminant, gamma, and viewing angle. To correct for these factors the colors are calibrated with a color reference chart. Due to the small camera window of the cameras a micro Color-Gauge target from IS_A was used to calibrate the colors. An ICC-profile is created based on the target measurement on one of the cameras, of which the color measurement used to create the color

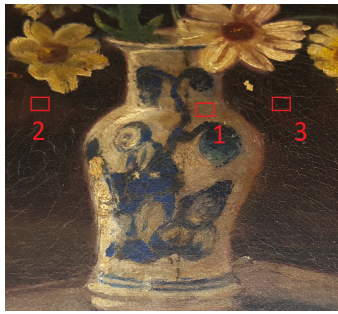


Figure 6: The paint sample with the three areas that are captured with the scanner and microscope. The areas have a size of 6.5x4.8 mm

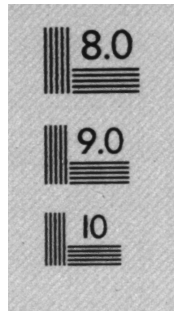


Figure 7: Detail of color image of MTF chart scan, showing the smallest features on the chart.

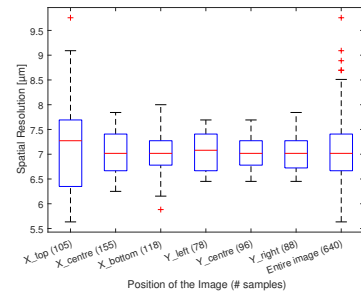


Figure 8: The spatial resolution in horizontal (X) and vertical (Y) orientated MTF bars dispersed over the image.

image corresponding to the height map. The color accuracy is measured with the standardized $\Delta E-2000$ metric, which quantifies the perceptual difference between two colors as observed by the human eye. The color values are extracted from the color corrected image of the micro color gauge and compared to the reference color value to compute the $\Delta E-2000$ for each color patch [SWD05] as well as the mean error over all patches.

4.5. Acquisition Time

The total acquisition time for a painting depends on: the amount of images per tile, the amount of tiles (depending also on the overlap between tiles), the exposure time and the movement time between the tiles. To determine the movement time and time it takes to capture one image (including the exposure time), the time stamp data of the complete scan of *Girl with a Pearl Earring* was used. The painting was captured with a exposure time of 0.6s. 308 tiles, with 13 images each were captured, with a 45 % overlap between the tiles.

4.6. Craquelure Analysis

The *Girl with a Pearl Earring* is used as a case study to determine the capability of our scanner to capture the craquelure of an entire painting. The topographical and color maps are combined to analyze the profile of the craquelure. 3D intersections of the craquelure are extracted from the scanning data to determine the width and depth of craquelure but also to visualize the profile of encountered cracks. The width and depth of craquelure are determined to validate whether the design requirements and current specifications are sufficient to accurately describe the craquelure pattern of a painting.

5. Results

5.1. Spatial Resolution

Figure 7 is a detail of the processed scan, meaning that this is the color image corresponding to the reconstructed 3D points of the surface, showing the finest features of the MTF chart (as shown in Figure 5). Figure 8 shows the spatial resolution for horizontal (X)

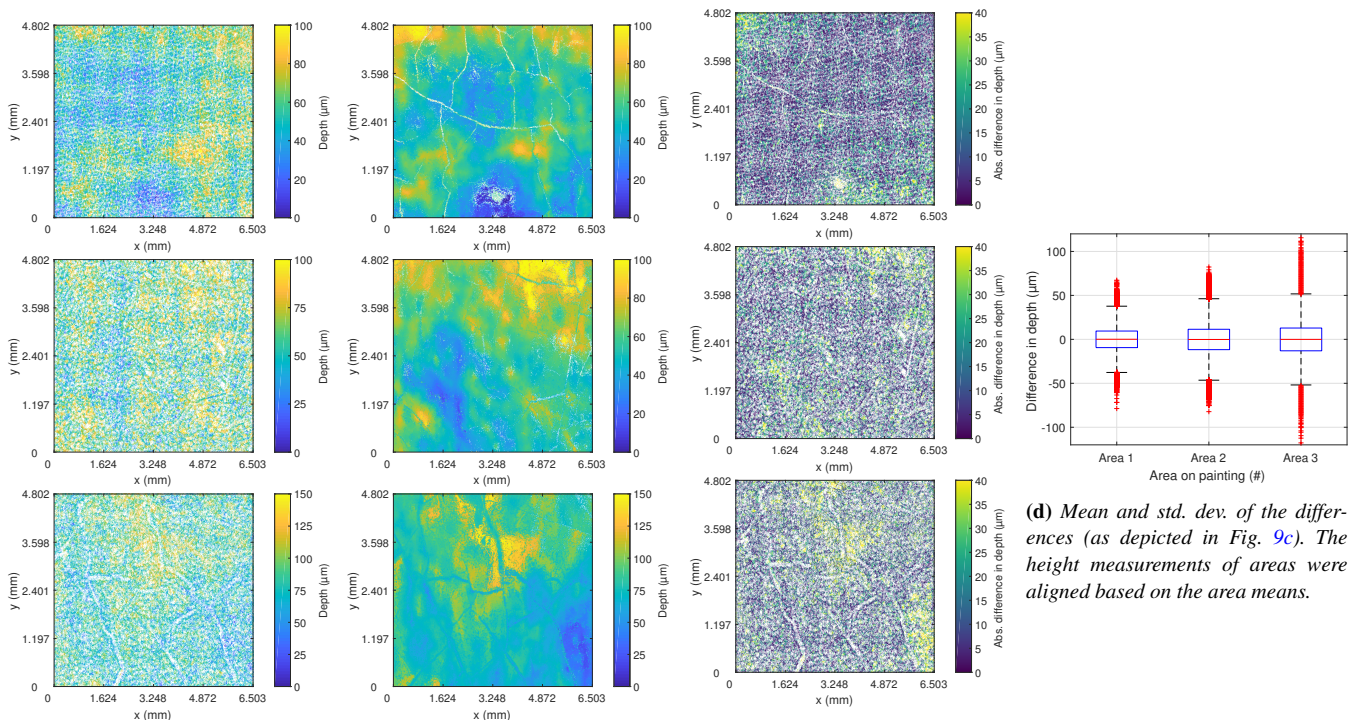
and vertical (Y) MTF bars dispersed over the processed image. The spatial resolution in X and Y direction do not significantly differ. Apart from the horizontal spatial resolution at the top of the image, the spread of the spatial resolution is similar for all areas of the image. The average spatial resolution over all the areas of the image, shown on the right side of the figure, is 7.03 μm ($\sigma = 0.49$, $n = 640$).

5.2. Depth accuracy

Figure 9 shows examples of the depth maps of our scanner and the Bruker ContourGT-K microscope of the same area of the sample of a painting (see Figure 6). The height maps of both devices are shown in Figure 9a and 9b showing the topography of the painting. The Bruker images are comprised of 3x3 stitched tiles, were as our sample region is taken from a single scan frame. White depicts pixels from which the height was not determined. The depth map from our scanner is less complete than the Bruker microscope, especially the performance of the depth estimation of the craquelure is less. However, the depth information is sufficiently dense to interpolate a complete depth map. Moreover, even the Bruker microscope suffers from not determined depth information. The absolute depth difference between our scanner and the Bruker is shown in Figure 9c. The standard deviation differs per area from 13 μm to 20 μm and over all areas the standard deviation is 17 μm (see Figure 9d). The depth accuracy is double the standard deviation, thus the average depth accuracy is 34 μm .

5.3. Color Accuracy

For scanning in complete darkness - using only the illumination of the projector - a exposure time of 2.0s was determined as the most ideal setting for the color calibration target. Figure 10 shows the color accuracy per color patch in the $\Delta E-2000$ metric for a exposure time of 2 seconds. The average $\Delta E-2000$ over the 30 color patches is 0.88 (max = 5.19), which meets the highest performance level for color imaging, as advised in the FADGI guidelines [Fed10]. For scanning the *Girl with a Pearl Earring*, due to incident environmental lighting, an exposure time of 0.6s was used and the color accuracy does not meet the digitization standards.



(a) Areas 1, 2 and 3 (see Figure 6) imaged with our scanner. Missing data is white. (b) Areas 1, 2 and 3 (see Figure 6) imaged with Bruker ContourGT-K microscope. Missing data is white. (c) Absolute difference between scanner and microscope measurement for areas 1, 2 and 3. Missing data is white. (d) Mean and std. dev. of the differences (as depicted in Fig. 9c). The height measurements of areas were aligned based on the area means.

Figure 9: The height maps of the scanner, from three regions on a test painting (see Figure 6), are compared to measurements of the Bruker ContourGT-K microscope to determine the depth accuracy.

1.51	0.21	0.70	0.53	0.60	0.52
0.87	1.32	0.51	0.17	0.52	0.34
0.90	0.15	0.31	0.74	0.60	0.98
0.33	0.48	5.19	3.41	1.53	0.32
0.61	0.65	0.51	0.32	0.61	1.17

Figure 10: The color accuracy expressed with the $\Delta E-2000$ metric for each color patch of the ColorGauge Micro Target.

5.4. Acquisition time

From the time stamp data of the scan of the *Girl with a Pearl Earring* it was determined that it takes 2.26 seconds to capture an image, excluding the time it takes to trigger the image itself (the exposure time). Besides that, it takes 3.4 seconds on average to move to the next scanning position. Given the dimensions of the painting, an exposure time of 2 seconds (suitable exposure time for a completely dark environment), and a scan strategy with 25% overlap, it is viable to scan a painting of these dimensions within 2 hours $((((2.26s+2s)*13 \text{ images}) + 3.4s)*120 \text{ tiles} = 1.9 \text{ hours})$.

5.5. Craquelure measurement on *Girl with a Pearl Earring*

Figure illustrates the selected area that is used for the 3D examples of the craquelure measured on the *Girl with a Pearl Earring* shown in figure . The 3D sections are enlarged and the height information is amplified to illustrate the profile of the craquelure examples. The ridge-shaped crack pattern, shown in Figure , is the most encountered type of craquelure. One side of the crack is elevated and has a sharp decrease in height to the other side. The expected rectangular shaped craquelure appears valley-shaped in our measurement, as shown in Figure and is less frequently encountered across the depth maps of the entire painting. The width of the ridge shaped craquelure is around 200 μm . The depth of the crack measured in the example varies from 20 to 80 μm .

6. Discussion

The results show that a 3D high resolution imaging device based on fringe encoded stereo imaging is an effective method to capture the surface of a painting in high resolution. The depth images from our scanner show clear correspondence to the microscopic 3D measurement (depicted in Figure 9). The height difference plot shows that the error is not randomly spread across the surface, whereby the largest errors are found in the extreme values. Further investigation is needed to determine the reason behind this deviation in measurement.

The spatial resolution of 7 μm is well below the required 10 μm . At this resolution, the scanner has the potential for research possibilities like monitoring the environmental influences on a painting or the analysis of brush strokes.

The depth accuracy has shown to be 34 μm , based on the chosen hardware and the specifications of the technique. The depth accuracy is currently insufficient to describe the three-dimensional shape of features which lie in the range of a single thin paint layer (estimated at 25 μm). If cracks with this depth magnitude occur in paintings, we will not be able to register them in terms of depth accuracy. However, an estimation of larger craquelure patterns, and the beginning of cracks thus the delamination can be registered. Moreover, the depth precision is better than all topography scanners for the entire surface of the painting mentioned in the literature study. To increase the depth accuracy, adding a third camera will resolve some of the trade-off between occlusion avoidance and depth accuracy. A third camera decreases the susceptibility to occlusions and increases the depth accuracy. Furthermore, the reduction in occlusions opens the possibility to increase the camera angle and thus the increase the depth resolution.

The color accuracy meets the FARGI guidelines when scanning in conditions without environmental lighting. In the case of scanning *Girl with a Pearl Earring* the lighting conditions were not ideal, with varying environmental lighting, which thereby lowers the color accuracy.

The analysis of the 3D information of *Girl with a Pearl Earring* showed that the profile of craquelure is more frequently an elevation resembling a ridge shape. The elevation might be explained by dirt that piled up in the crack during one of the restorations [Deu08] or that the paint layers curve upwards at crack edge due to delamination at the edges. The craquelure that did have an valley shaped profile rather approximates a convex shape than the expected right angled rectangular shape, which might be the result of occlusions from stereo imaging. As mentioned, both cameras need to register the same area to determine the depth and is therefore sensitive to occlusions in craquelure, which make the profile more valley shaped. It requires more research to determine the exact measurement, type and origin of the profile of the craquelure. The 3D digitization of paintings surface will aid the classification of craquelure patterns in further research [Buc00], in combination with new digital extraction and visualization techniques [LTPH17].

Furthermore, the main drawback of increasing the resolution is a proportional reduction of the depth of field, increasing the difficulty to focus the images of both cameras. The images have to be in focus sufficiently to be able to match the features of both images and to accurately compute the depth map. The minimal required amount of focus for fringe encoded stereo imaging to compute the depth map should be investigated in future research.

7. Conclusion

In this paper, we presented a high resolution color and topography scanner capable of capturing the craquelure pattern of *Girl with a Pearl Earring*. We replaced the hardware and software of the latest scanner based on fringe encoded stereo imaging to increase the spatial resolution, the depth accuracy, whilst retaining an acceptable

acquisition speed. Experimental validations show that the scanner reaches a spatial resolution of 7 μm and a depth precision of 34 μm . The performance of digitally reproducing the color information accurately satisfies the digitization guidelines of FADGI [Fed10].

A scan of *Girl with a Pearl Earring* indicates that a minimum acquisition time of 40 seconds per tile is required, resulting in an acquisition time of 2 hours for a painting of 39x44.5 cm with a 25% overlap and 2 seconds exposure time. The scans determined that the profile of the craquelure rarely has the expected valley shape. The profile of craquelure rather frequently has an elevated profile approximating a ridge shape. The origin and variation of craquelure profiles display an interesting path for future research.

The potential addition of a third camera, and a reconfiguration of the existing two cameras, in combination with further development in image processing, provides the potential for further improvement in depth resolution, needed to capture the finest surface features in a painting. A scanning system based on fringe encoded multi-camera vision, can provide an valuable addition to 3D microscopy, to document and monitor the three-dimensional shape of a complete painting in a fraction of the acquisition time.

8. Acknowledgment

The authors would like to thank Océ Technologies, a Canon company, for sponsoring the hardware required to develop the high resolution scanner. The data presented in this paper was gathered as part of the research project *The Girl in the Spotlight*, a Mauritshuis initiative, led by paintings conservator Abbie Vandivere, with a team of internationally recognized specialists working within the collaborative framework of the Netherlands Institute for Conservation, Art and Science (NICAS). The *Girl in the Spotlight* research project was made possible with support from the Johan Maurits Compagnie Foundation.

References

- [ASC*13] ARBACE L., SONNINO E., CALLIERI M., DELLEPIANE M., FABBRI M., IDELSON A. I., SCOPIGNO R.: Innovative uses of 3d digital technologies to assist the restoration of a fragmented terracotta statue. *Journal of Cultural Heritage* 14, 4 (2013), 332–345. doi: 10.1016/j.culher.2012.06.008. 2
- [BBC18] BBC: The secrets of girl with a pearl earring. 2018. URL: <http://www.bbc.com/culture/story/20180314-the-secrets-of-girl-with-a-pearl-earring>. 2
- [BCD*92] BURMESTER A., CUPITT J., DERRIEN H., DESSIPRIS N., HAMBER A., MARTINEZ K., MÜLLER M., SAUNDERS D.: The examination of paintings by digital image analysis. In *Proc. 3rd Int. Conf. Non-Destructive Testing, Microanalytical Methods and Environmental Evaluation for Study and Conservation of Works of Art* (1992), pp. 201–214. 2
- [BFM*13] BARBETTI I., FELICI A., MAGRINI D., MANGANELLI DEL FA R., RIMINESI C.: Ultra close-range photogrammetry to assess the roughness of the wall painting surfaces after cleaning treatments. *International Journal of Conservation Science* 4 (2013). 3
- [BP03] BARSKY S., PETROU M.: The 4-source photometric stereo technique for three-dimensional surfaces in the presence of highlights and shadows. *IEEE Transactions on Pattern Analysis and Machine Intelligence* 25, 10 (2003), 1239–1252. 3

- [Bra86] BRACEWELL R.: *The Fourier transform and its applications*. McGraw-Hill New York, 1986. 2
- [Bru18] BRUKER INC.: ContourGT-K 3d optical microscope datasheet, May 2018. URL: <https://www.bruker.com/products/surface-and-dimensional-analysis/3d-optical-microscopes/contourg-t-k/overview.html>. 6
- [BTC*] BLAIS F., TAYLOR J., COURNOYER L., PICARD M., BORGEAT L., GODIN G., BERALDIN J.-A., RIOUX M., LAHANIER C.: Ultra high-resolution 3d laser color imaging of paintings: The Mona Lisa by Leonardo Da Vinci. In *7th International Conference on Lasers in the Conservation of Artworks*, National Research Council Canada. 2
- [Buc97a] BUCKLOW S.: The description of craquelure patterns. *Studies in Conservation* 42, 3 (1997), 129–140. 2
- [Buc97b] BUCKLOW S. L.: A stylometric analysis of craquelure. *Computers and the Humanities* 31, 6 (1997), 503–521. 2
- [Buc00] BUCKLOW S.: Consensus in the classification of craquelure. *Hamilton Kerr Institute Bulletin* 3 (2000), 61–73. 2, 9
- [CSKH90] CURCIO C. A., SLOAN K. R., KALINA R. E., HENDRICKSON A. E.: Human photoreceptor topography. *Journal of comparative neurology* 292, 4 (1990), 497–523. 3
- [Deu08] DEURENBERG R. M.: Examination and treatment of a set of klismos chairs, attributed to john and hugh finlay. *Journal of the American Institute for Conservation* 47, 2 (2008), 97–117. 9
- [EEL*17] ELKHUIZEN W. S., ESSERS T. T. W., LENSEIGNE B., WEJKAMP C., SONG Y., PONT S. C., GERAEDTS J. M. P., DIK J.: Reproduction of Gloss, Color and Relief of Paintings using 3D Scanning and 3D Printing. In *Eurographics Workshop on Graphics and Cultural Heritage* (2017). doi:10.2312/gch.20171312. 3, 4, 5
- [EZV*14] ELKHUIZEN W. S., ZAMAN T., VERHOFSTAD W., JONKER P. P., DIK J., GERAEDTS J. M.: Topographical scanning and reproduction of near-planar surfaces of paintings. In *Electronic Imaging* (2014), vol. 9018, IS&T/SPIE. doi:10.1117/12.2042492. 2
- [Fed10] FEDERAL AGENCIES DIGITIZATION INITIATIVE: Technical guidelines for digitizing cultural heritage materials: creation of raster image master files, 2010. 3, 7, 9
- [FKK*07] FUJITA K., KOBAYASHI M., KAWANO S., YAMANAKA M., KAWATA S.: High-resolution confocal microscopy by saturated excitation of fluorescence. *Physical review letters* 99, 22 (2007), 228105. doi:10.1103/PhysRevLett.99.228105. 3
- [JBC96] JANE S., BARKER R., CHAD J.: Confocal microscopy and art conservation. *Microscopy and Analysis* 31, 55 (1996). 1
- [Lau05] LAUDENBACHER K.: Reentelado, parches y remiendos: mucha tela. In *Interim meeting, international conference on painting conservation: canvases, behaviour, deterioration and treatment* (2005), Editorial UPV, pp. 111–118. 2
- [Lel96] LELEKOVA O.: Expert examination of icons. In *ICOM committee for conservation, 11th triennial meeting in Edinburgh, Scotland, 1-6 September 1996* (1996), James & James, pp. 367–370. 2
- [Low04] LOWE D. G.: Distinctive image features from scale-invariant keypoints. *International journal of computer vision* 60, 2 (2004), 91–110. 6
- [LRKH06] LUHMANN T., ROBSON S., KYLE S., HARLEY I.: *Close range photogrammetry: principles, techniques and applications*. Whitlles Publishing, 2006. 3
- [LTPH17] LAWONN K., TROSTMANN E., PREIM B., HILDEBRANDT K.: Visualization and extraction of carvings for heritage conservation. *IEEE transactions on visualization and computer graphics* 23, 1 (2017), 801–810. doi:10.1109/TVCG.2016.2598603. 9
- [Mau94] MAURITSHUIS: Sample during treatment: Girl with a pearl earring. Unpublished research, 1994. 2
- [MP04] MÄENPÄÄ T., PIETIKÄINEN M.: Classification with color and texture: jointly or separately? *Pattern recognition* 37, 8 (2004), 1629–1640. 2
- [OBSG10] OBERTHALER E., BOON J. J., STANEK S., GRIESSER M.: *Die Malkunst Spurensicherung an einem Meisterwerk: Ausstellungskatalog des Kunsthistorischen Museums Wien*. Residenz Verlag, 2010, ch. The Art of Painting by Johannes Vermeer. History of treatments and observations on the present condition. 2
- [Oka97] OKANO Y.: MTF analysis and its measurements for digital still camera. In *IS&T 50th annual conference* (1997), The society for imaging science and technology, pp. 383–387. 6
- [OS17] OWENS B., SCOTT A. R.: Software: Picture perfect. *Nature* 545, 7654 (2017), S12–S12. 3
- [Pho17] PHOTOMODELER: Factors affecting accuracy in photogrammetry, 2017. URL: https://info.photomodeler.com/blog/kb/factors_affecting_accuracy_in_photogrammetry/. 3
- [Roc05] ROCHE A.: Comportement mécanique des peintures sur toile: évaluation de la stabilité mécanique aux variations d’humidité et de température. In *Interim meeting, international conference on painting conservation: canvases, behaviour, deterioration and treatment* (2005), Editorial UPV, pp. 189–212. 2
- [SJ13] STUB JOHNSEN J.: Conservation of cultural heritage, european standards on the environment. In *Munich Climate Conference, Climate for Collections Standards and Uncertainties* (2013), Archetype Publications Ltd., pp. 35–44. URL: http://www.doernerinstitut.de/downloads/Climate_for_Collections.pdf. 2
- [SR13] STONER J. H., RUSHFIELD R.: *Conservation of Easel Paintings*. Routledge, 2013. 2
- [SSD08] SHAHRAM M., STORK D. G., DONOHO D.: Recovering layers of brush strokes through statistical analysis of color and shape: an application to van gogh’s self portrait with grey felt hat. In *Electronic Imaging* (2008), vol. 6810. doi:10.1117/12.765773. 2
- [SSd*09] STROO C., SYFER-D’OLNE P., DUBOIS A., SLACHMUYLDERS R., D’OLNE P., FRANSEN B., PETERS F.: *The Flemish Primitives: catalogue of early Netherlandish painting in the Royal Museums of Fine Arts of Belgium*, vol. 1-5. Brepols Publishers, 1996-2009. 3
- [SWD05] SHARMA G., WU W., DALAL E. N.: The CIEDE2000 color-difference formula: Implementation notes, supplementary test data, and mathematical observations. *Color Research & Application* 30, 1 (2005), 21–30. doi:10.1002/col.20070. 7
- [Tow94] TOWNSEND J. H.: Microscopy and paintings. *Microscopy and analysis* 39 (1994), 11–13. 3
- [Van18a] VANDIVERE A.: Girl with a blog, 2018. URL: <https://www.mauritshuis.nl/en/explore/restoration-and-research/girl-with-a-blog/>. 2
- [Van18b] VANDIVERE A.: Up close and personal, 2018. URL: <https://www.mauritshuis.nl/en/explore/restoration-and-research/girl-with-a-blog/14-up-close-and-personal/>. 1, 3
- [Woo80] WOODHAM R. J.: Photometric method for determining surface orientation from multiple images. *Optical engineering* 19, 1 (1980). doi:10.1117/12.7972479. 3
- [Zam13] ZAMAN T.: *Development of a topographical imaging device for the near-planar surfaces of paintings*. Master’s thesis, Delft University of Technology, 2013. 4, 5
- [Zha00] ZHANG Z.: A flexible new technique for camera calibration. *IEEE Transactions on pattern analysis and machine intelligence* 22, 11 (2000), 1330–1334. 5
- [ZJLD14] ZAMAN T., JONKER P., LENSEIGNE B., DIK J.: Simultaneous capture of the color and topography of paintings using fringe encoded stereo vision. *Heritage Science* 2, 1 (2014), 23. 2, 3, 6